Biogeosciences

Sedimentary organic matter and carbonate variations in the Chukchi Borderland in association with ice sheet and ocean-atmosphere dynamics over the last 155 kyr

S. F. Rella and M. Uchida

National Institute for Environmental Studies, Environmental Chemistry Division, AMS facility NIES-TERRA,
Onogawa 16-2, Tsukuba 305-8506, Japan

Abstract. Knowledge on past variability of sedimentary organic carbon in the Arctic Ocean is important to assess natural carbon cycling and transport processes related to global climate changes. However, the late Pleistocene oceanographic history of the Arctic is still poorly understood. In the present study we show sedimentary records of total organic carbon (TOC), $CaCO_3$, benthic foraminiferal $\delta^{18}O$ and the coarse grain size fraction from a piston core recovered from the northern Northwind Ridge in the far western Arctic Ocean, a region potentially sensitively responding to past variability in surface current regimes and sedimentary processes such as coastal erosion. An age model based on oxygen stratigraphy, radiocarbon dating and lithological constraints suggests that the piston core records paleoenvironmental changes of the last 155 kyr. TOC shows orbital-scale increases and decreases that can be respectively correlated to the waxing and waning of large ice sheets dominating the Eurasian Arctic, suggesting advection of fine suspended matter derived from glacial erosion to the Northwind Ridge by eastward flowing intermediate water and/or surface water and sea ice during cold episodes of the last two glacial-interglacial cycles. At millennial scales, increases in TOC might correlate to a suite of Dansgaard-Oeschger Stadials between 120 and 45 ka before present (BP) indicating a possible response to abrupt northern hemispheric temperature changes. Between 70 and 45 ka BP, closures and openings of the Bering Strait could have additionally influenced TOC variability. $CaCO_3$ content tends to anti-correlate with TOC on both orbital and millennial time scales, which we interpret in terms of enhanced sediment advection from the carbonate-rich Canadian Arctic via an extended Beaufort Gyre during warm periods of the last two glacial-interglacial cycles and increased organic carbon advection from the Siberian Arctic during cold periods when the Beaufort Gyre contracted. We propose that this pattern may be related to orbital- and millennial-scale variations of dominant atmospheric surface pressure systems expressed in mode shifts of the Arctic Oscillation.

1 Introduction

The causes and implications of recent climate change are intensively debated. In particular the Arctic region appears to respond sensitively to climate change, as demonstrated by a near-continuous decrease in annual sea ice extent over the last 30 yr (Johannessen et al., 2004). Arctic environmental change directly relates to changes in total organic carbon (TOC) in Arctic Ocean sediments through variable terrestrial and marine input of organic matter. Today, coastal erosion and to a lesser extent large rivers such as the Yenisei and Lena play the dominant role for terrestrial organic carbon (OC_{terr}) input along the coasts of Siberia and Alaska (Reimnitz et al., 1988; Rachold et al., 2000). In the Canadian Beaufort Sea, on the other hand, river discharge from the Mackenzie River is more important than coastal erosion (Macdonald et al., 1998). Marine organic carbon (OC_{mar}) accumulation is mainly limited by the extents of sea ice, which decreases surface productivity by one order of magnitude compared to open water conditions (Wollenburg and Mackensen, 1998). Thus, past variations in TOC deposition in Arctic Sea sediments provide a sensitive tool for tracking environmental changes that can be related to processes at land and sea, such as glacial erosion by ice sheets, river discharge, ocean circulation patterns and marine productivity. However, the orbital-to millennial-scale TOC variations in the far western and far eastern Arctic are poorly known, despite their importance for our understanding of sedimentary processes in relation to environmental change, for example through openings and closures of the Bering Strait (Hu et al., 2010). Here we present

records of TOC and calcium carbonate ($CaCO_3$) over the last 155 000 yr (155 kyr) from a sediment core recovered from the northern Northwind ridge, an area potentially strongly responding to climate change through changing ocean currents such as the Beaufort Gyre, summer sea ice extent, as well as variable organic matter supply.

2 Present and past oceanographic setting

The Chukchi Borderland, located about 1000 km north of the Bering Strait, is characterized by a complex topography of ridges and plateaus, which extend northward from the Chukchi Shelf into the Amerasian Basin (Fig. 1). Today, the area is primarily influenced by Pacific waters entering through the Bering Strait and a clockwise current in the Canada Basin known as Beaufort Gyre (e.g. Macdonald et al., 2003). The Beaufort Gyre transports sea ice and sediments from the Canadian Arctic to the Central Arctic (Stein, 2008). As a result of nutrient-rich Pacific water influx and open waters in summers, the contribution of OC_{mar} in the surface sediments of the Chukchi Borderland is relatively high (50 % of TOC) (Naidu et al., 2004; Belicka and Harvey, 2009), compared to common average values of 10 to 20 % in the Arctic Ocean due to significant input of OC_{terr} from the surrounding continents (Stein, 2008) (Fig. 1). At depths between ∼200 and ∼800 m, the Chukchi Borderland is influenced by the so called Atlantic Layer, an intermediate water mass inflowing from the Atlantic into the Arctic Ocean along the slopes of the Eurasian shelves (Fig. 1). Beneath the Atlantic Layer deep bottom water fills the Amerasian and Eurasian Basin.

The adjacent Chukchi Shelf encompasses an area of 620×10^3 km^2 with a mean depth of ∼80 m. Due to its shallow depth the Chukchi Shelf was largely exposed during the Last Glacial Maximum (LGM) ca. 22 000 to 19 000 yr before present (22 to 19 ka BP), when sea level was ∼120 m lower than today (Fig. 1). During Marine Isotope Stage (MIS) 2, 6, and partly MIS 3 and 4 the Bering Strait was closed (Hu et al., 2010) owing to its shallow depth of only ∼50 m today, inhibiting the inflow of Pacific waters.

During glacial periods large ice sheets dominated the shelves and adjacent land of western Siberia, the Canadian Arctic and Greenland (Dowdeswell et al., 2002). These ice sheets played an important role in transporting sediments to the shelf break through glacial erosion, sediment mass wasting (Dowdeswell et al., 1998, 2002) and calving of icebergs (e.g. Josenhans et al., 1986; Shipp et al., 2002). A fraction of the sediments is further transported from the shelf break of the Barents and Kara seas far to the east via the Atlantic Layer (Knies et al., 2001). Sea ice drifting transports sediments along prevailing surface currents, which depend on dominant wind patterns (e.g. Bischof and Darby, 1997).
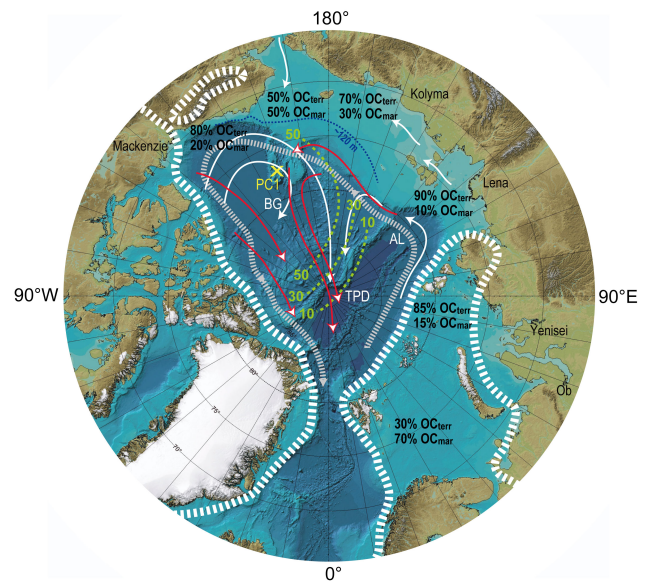

Fig. 1. Map of the Arctic Ocean and adjacent land masses. Location of PC1 is indicated by an "x". Modern surface currents, typical for warm periods and a negative Arctic Oscillation (AO) mode are shown as white arrows (BG = Beaufort Gyre; TPD = Transpolar Drift), proposed surface currents during cold periods and a positive AO mode are shown as red arrows (after Darby and Bischof, 2004). The Atlantic Layer (AL) intermediate water flow is indicated as dashed grey arrow. The white dashed lines denote extents of reconstructed LGM ice sheets (Svendsen et al., 2004). The names of large rivers are indicated at their present location. Modern average percentages of terrestrial and marine organic carbon on the Arctic shelves are also shown (after Stein et al., 2008). The green dashed lines delineate isolines of carbonate percentages (indicated as green numbers) in Arctic sediments (data from Phillips and Grantz, 2001). The ∼120 m isobath in the Chukchi Borderland region is drawn as a blue dashed line.

3 Methodology

3.1 Core location and description

Piston core MR08-04 PC1 has been recovered in summer 2008 at 998 m water depth from the northern part of the Northwind Ridge (74°48.50′ N, 158°31.85′ W) (Fig. 1). Based on visual core inspection and soft X-ray radiographs, taken using a SOFTEX PRO-TEST 150, the core mainly consists of grey to olive brown clayey sediments (Fig. 2a). A light brown interval can be observed between 535 and 575 cm depth and two pink-whitish layers between 652 and 655, and 669 and 672 cm depth. A whitish layer is also recognized between 447 and 449 cm depth. Millimeter-scale laminations occur between 17 and 51 cm, and mm- to cm-scale laminations between 638 and 646, and 683 and 690 cm depth. PC1 is also characterized by several layers of mm-scale scattered IRD and isolated cm-scale IRD clasts (Fig. 2a).
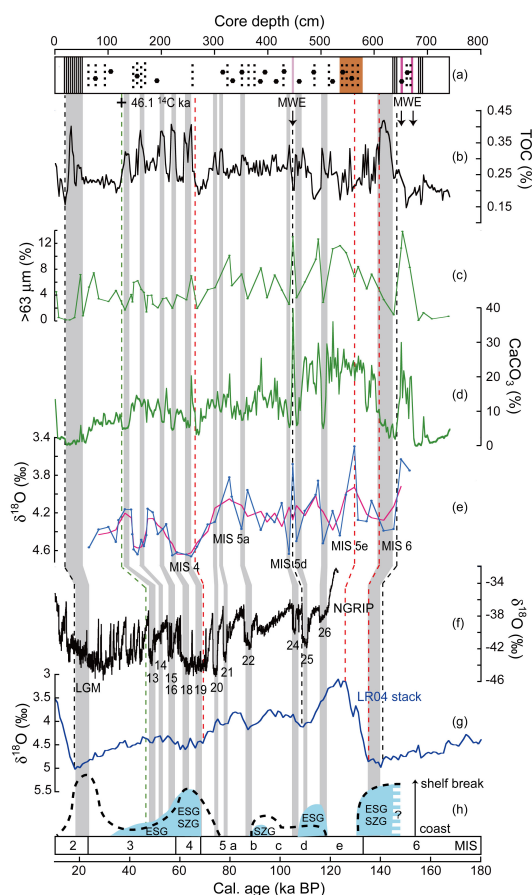
Fig. 2. Variations in **(a)** the lithology of PC1, **(b)** TOC of PC1, **(c)** the > 63 μm fraction of PC1, **(d)** CaCO$_3$ of PC1 and **(e)** benthic δ^{18}O of PC1 (overlap is the 3-point moving average) with core depth, and temporal variations in **(f)** the NGRIP δ^{18}O record (NGRIP members, 2004), **(g)** the benthic LR04 δ^{18}O stack (Lisiecki and Raymo, 2005), and **(h)** the extent of Eurasian ice sheets between the coast and the shelf break (Knies et al., 1999, 2000; Müller et al., 1999). In the columnar section of PC 1 (panel a), the large black dots represent IRD clasts, the small black dots are scattered IRD and vertical black lines indicate laminated horizons based on visual core inspection and soft-X ray radiographs. The light brown layer between 535 and 575 cm, as well as the pink-whitish layers at ~653 and ~670 cm and the whitish layer at ~448 cm depth possibly associated with meltwater events (MWE) are also shown. Extents of the East Siberian Glaciation (ESG) and the Severnaya Zemlya Glaciation (SZG) are presented as blue shadings (panel h). Extents of the Northern Barents Sea Ice Sheet are indicated as dashed black line (panel h). MIS stages are shown on top of the calendar age scale. Red dashed lines, the green dashed line, and the black dashed lines indicate the proposed correlation between the LR04 δ^{18}O stack and the benthic δ^{18}O record of PC1, the age-depth correlation based on radiocarbon dating, and the age-depth correlation based on lithological constraints, respectively. Vertical grey shadings indicate relative increases of TOC and their possible relation to DOS and/or MIS stages. Corresponding stadial numbers are shown in panel (f).

3.2 Carbon measurements

Core PC1 was subsampled at 2.3 cm resolution. For the measurement of bulk carbon (C) contents, 1 to 1.5 g of freeze-dried sediments per sample were powdered, wrapped in tin capsules and measured using a CHN analyzer (EA1112, EURO SCIENCE) at the National Institute for Environmental Studies in Tsukuba. For TOC measurements, 1 g sediment per sample was treated with 1N HCL overnight to dissolve CaCO$_3$, washed three times using distilled water and dried in an oven overnight at 50 °C prior to powdering and measurement by the CHN analyzer. The percentage of CaCO$_3$ in the sediments has been approximated using the equation

$$\%CaCO_3 = (\%C - \%TOC) \times (100/12) \qquad (1)$$

where the factor 100/12 corresponds to the atomic weight ratio of CaCO$_3$ and C.

3.3 Benthic oxygen isotope measurements

In order to reconstruct temporal changes of bottom water oxygen isotopes at site PC1, 53 samples were selected at 5 to 20 cm intervals throughout the core, wet-sieved over a 63 μm sieve, rinsed in distilled water, dried overnight at 50 °C and weighed for an estimation of the coarse (> 63 μm) fraction. Using a binocular microscope, 3 to 10 species of *Bulimina aculeata*, which calcifies its test close to the calcite oxygen isotope equilibrium (McCorkle et al., 1997), were hand-picked from the > 150 μm fraction of each sample. Foraminifera were analyzed at the Bloomsbury Environmental Isotope Facility of the University College London. Oxygen isotopic data were expressed in standard δ notation relative to the Peedee Belemnite (PDB) carbonate standard with an instrumental precision of < 0.06 ‰.

3.4 Radiocarbon measurements

To constrain sediment ages in the upper part of PC1, we measured radiocarbon (^{14}C) contents of the planktonic foraminifera *Neogloboquadrina pachyderma* at 122.6 and 125 cm depth. Sediment samples were wet-sieved over a 63 μm screen, rinsed in distilled water and dried overnight at 50 °C. Foraminifera were hand-picked, cleaned by soaking in a 30 % H$_2$O$_2$ solution to remove adhering contaminants, and converted to CO$_2$ by dissolution in 100 % phosphoric acid (H$_3$PO$_4$) in evacuated glass tubes. The CO$_2$ gas was cryogenically purified, reduced to graphite over an iron catalyst in the presence of H$_2$ and subsequently submitted to radiocarbon dating at the AMS facility (NIES-TERRA) of the National Institute for Environmental Studies, Tsukuba (Uchida et al., 2004, 2005, 2008).

4   Results

4.1   Age model

To construct an age model we relied on a comparison of our benthic $\delta^{18}O$ record with the global benthic $\delta^{18}O$ stack LR04 (Lisiecki and Raymo, 2005) (Fig. 2g), radiocarbon dating of planktonic foraminifera and on changes in colour and lithology of the sediments in PC1. Variations in benthic $\delta^{18}O$ are a function of changes in global ice volume, bottom water salinity and bottom water temperature. Because the Arctic Ocean is a semi-enclosed basin and $\delta^{18}O$ may be more readily influenced by salinity and temperature changes, for example in response to meltwater events, a detailed correlation to the LR04 $\delta^{18}O$ stack should be considered with care. Restricting ourselves to major features, we nevertheless recognize that benthic $\delta^{18}O$ values below ~300 cm depth are on average lighter than in the upper part of the core, suggesting that the lower part was mostly deposited during an interglacial period. Furthermore, the major transition from the last interglacial to the last glacial stage (from MIS 5 to MIS 4), as documented in the LR04 benthic $\delta^{18}O$ stack, seems to be well resolved in our benthic $\delta^{18}O$ record between 230 and 330 cm depth (Fig. 2e, g). We suggest that the lightest $\delta^{18}O$ values at 563 cm depth could be correlated to MIS 5e in view of the occurrence of a brownish layer in the same interval, which is indicative for peak interglacial conditions in sediments of the Arctic Ocean (e.g. Phillips and Grantz, 1997). Glacial deposits, on the other hand, are typically of more greyish colour, and characterized by a low degree of bioturbation or laminations (absence of bioturbation) (Stein, 2008). Laminations may be expected in particular during glacial maxima such as MIS 2 and MIS 6 in the western Arctic Ocean, as such periods were probably characterized by perennial sea ice cover (Darby et al., 1997) and strongly limited benthic fauna (Wollenburg and Mackensen, 1998). We therefore correlate the laminations near core top and those near core bottom to MIS 2 and MIS 6, respectively. The light $\delta^{18}O$ values at ~660 cm depth, which are lithographically positioned between the two laminated layers near core bottom, would thus probably have occurred during late MIS 6 and may have been related to a late glacial meltwater event from the Canadian Arctic judging from its association with two pink-white layers and percentage peaks in $CaCO_3$ and the coarse fraction (Fig. 2a, c–e). Late MIS 6 meltwater events were also reported by Spielhagen et al. (2004) on the Alpha Ridge. Coeval spikes in $\delta^{18}O$, $CaCO_3$ and coarse fraction associated with a whitish layer in PC1 are also observed at ~448 cm depth (Fig. 2a, c–e), and may similarly suggest a meltwater event from the Canadian Arctic. We thus tentatively correlate this event to the Canadian Arctic sourced meltwater events reported from the Mendeleev Ridge (Polyak et al., 2004) and Alpha Ridge (Spielhagen et al., 2004) during MIS 5d (~110 ka BP) in consistency with lithological and oxygen stratigraphic con-

straints of our age model (Fig. 2). Radiocarbon dating on *N. pachyderma* yielded ^{14}C ages of 46.6 ± 0.4 ka (TERRA-090809a37) and 45.6 ± 0.5 ka (TERRA-090809a34) at 122.6 and 125 cm depth, respectively. Recalculation of ^{14}C ages based on the Intcal09/Marine09 calibration curve (Reimer et al., 2009) using the CALIB 6.0 software (Stuiver and Reimer, 1993) suggests calendar ages of respectively 47.3 ± 0.6 (2σ) ka BP and 46.4 ± 1.4 (2σ) ka BP. The average calendar age of 46.9 ± 1.4 ka BP at ~123.8 cm depth is well consistent with our age estimation based on oxygen stratigraphy for this depth interval. According to this age model, the sedimentation rate of core PC1 is relatively constant at ~5 cm/kyr, which is a reasonable value for cores recovered from ridges such as the Northwind Ridge in the Arctic Ocean for the last glacial-interglacial cycle (e.g. Backman et al., 2004).

4.2   Downcore variations of TOC, $CaCO_3$ and coarse fraction

The variation of TOC in PC1 is shown in Fig. 2b. TOC values range between ~0.15 and ~0.45 %, punctuated by major peaks centered at 618, 584, 502, 250, 223, 201, 161, 135 and 35 cm depth. Between 447 and 292 cm values are generally elevated ranging between ~0.25 and ~0.3 % including several low amplitude peaks reaching ~0.35 %.

Variation of $CaCO_3$ with depth is presented in Fig. 2d. $CaCO_3$ is low between core bottom and 676 cm, and between 65 cm and core top with values ranging from ~0.2 to ~5 %. Between 602 and 461 cm, $CaCO_3$ is high ranging from 10 to 36 % and averaging ~22 %, except for a negative excursion at ~504 cm, where values decrease to 5 %. Between 461 and 70 cm, $CaCO_3$ averages ~11 %, but shows a high peak of 40 % at 447 cm and cyclically increased values (~8 to ~20 %) between 420 and 374, 330 and 292, 212 and 151, and 125 and 76 cm. Between these layers of increased values, $CaCO_3$ is relatively low ranging from ~5 to ~10 %. Temporal variations in the coarse fraction in PC1 (Fig. 2c) are similar to $CaCO_3$, which is also expressed in a high correlation coefficient of $R^2 = 0.71$ for the two variables. Preliminary inspection of planktonic and benthic foraminifer contents suggests that biogenic carbonate constitutes between 0 and 5 % of the sample amount and that most of the $CaCO_3$ variation in PC1 should be regarded detrital in nature.

5   Discussion

5.1   Variations of TOC, $CaCO_3$ and coarse fraction in relation to global ice volume changes

Changes in global ice volume are largely represented by benthic $\delta^{18}O$ stacks such as the LR04 benthic stack (Lisiecki and Raymo, 2005) (Fig. 2g). $\delta^{18}O$ maxima between 140 and 135 ka BP (late MIS 6) and between 25 and 18 ka BP (MIS 2) are associated with distinct increases in TOC at site PC1

(Fig. 2b), while $CaCO_3$ and the coarse fraction show low values during these intervals (Fig. 2c, d). The ice volume advances during MIS 5d and 4 (Fig. 2g) similarly correspond to increased TOC and generally decreased $CaCO_3$ and coarse fraction contents, although both $CaCO_3$ and the coarse fraction show a millennial-scale peak during MIS 5d, which is probably related to a meltwater event as outlined in chapter 4.1. MIS 5b, on the other hand, is associated with only small amplitude TOC increases, but distinct minima in $CaCO_3$ and the coarse fraction. Relatively low TOC and relatively high $CaCO_3$ and coarse fraction contents correspond to periods of decreased ice volume during MIS 5e, 5c and 5a, but can be also identified for the period between 45 and 25 ka BP.

5.2 Variations of TOC and $CaCO_3$ in relation to temperature changes in the high latitude Northern Hemisphere

Variations of $\delta^{18}O$ in the NGRIP ice core (NGRIP members, 2004) (Fig. 2f) reflect air temperature changes in the high latitude Northern Hemisphere. The millennial-scale abrupt temperature fluctuations during the last glacial period (Dansgaard-Oeschger Cycles, DOC) recorded in NGRIP indicate dramatic climate changes in response to internal climate feedbacks, possibly modulated by variations in solar forcing (Braun et al., 2005). A close comparison of our data with the NGRIP ice core might suggest that millennial-scale increases in TOC might be correlated to Dansgaard-Oeschger Stadials (DOS) 26 to 24, 22 to 18, as well as DOS 15/16, 14 and 13 (Fig. 2b, f). DOS 18 and 13 correspond to Heinrich events H6 and H5 (e.g. Hemming, 2004). On the basis of this correlation, decreases in $CaCO_3$ might correlate to DOS 26 to 24, 22, 19, 18, 15/16, and 13 (Fig. 2d, f). It should be noted, however, that these correspondences are still speculative and associated with considerable uncertainties due to unknown millennial-scale sedimentation rates and the nature of our age model, which is only constrained on orbital scales. The good temporal correspondence of increases in TOC and decreases in NGRIP $\delta^{18}O$, however, seems to suggest that millennial-scale variations in TOC could be related to abrupt temperature changes in the high latitude Northern Hemisphere.

5.3 Orbital-scale TOC variations in response to ice sheet dynamics

The last two glacial-interglacial cycles were characterized by a dynamic waxing and waning of large ice sheets in the Arctic (e.g. Knies et al., 1999, 2000; Müller et al., 1999). For instance, during the global ice sheet advances MIS 6, 4 and 2, voluminous ice sheets covered the land and adjacent shelves of the western Eurasian Arctic, the Canadian Arctic and Greenland (Figs. 1 and 2h). TOC contents in Arctic Ocean sediments in relative proximity to the western Siberian Arctic show distinct increases during these time intervals, which can be well correlated between sediment cores (e.g. Winkelmann et al., 2007, 2008). Primary processes for land-ocean transport of OC_{terr} in the Arctic Ocean are coastal erosion and river discharge (Reimnitz et al., 1988; Rachold et al., 2000; Stein, 2008), importantly supplemented during glacial periods by bedrock-eroded material carried by ice streams and ice sheet flows to the shelf edge (e.g. Elverhøi et al., 1998, Dowdeswell et al., 2002). OC_{terr} is further transported by surface and deep currents, sea ice and icebergs to the open ocean (Stein and Korolev, 1994).

TOC values at site PC1 are generally low, but nonetheless characterized by distinct peaks, in particular during MIS 6, 4 and 2. These results are consistent with a study from the nearby Mendeleev Ridge, where increased input of terrestrial organic matter was observed during cold periods associated with more efficient transport of organic matter from the land to the ocean (Yamamoto and Polyak, 2009). Yamamoto and Polyak (2009) also suggested that transport of terrestrial organic matter during cold episodes was associated with fine and muddy sediments at the Mendeleev Ridge as also observed in our record, where increases in TOC are mostly associated with low coarse fractions (Fig. 2b, c). These observations also suggest that TOC increases at PC1 during cold periods occur dominantly due to OC_{terr} supply rather than OC_{mar}, which would more likely increase during warm periods (Wollenburg and Mackensen, 1998).

We accordingly propose that a fraction of bedrock-derived organic material delivered to the shelf breaks of the Eurasian Arctic due to glacial erosion during MIS 6, 4 and 2 was transported eastward to the Chukchi Borderland as fine suspended matter under the influence of eastward flowing intermediate waters of the Atlantic Layer and/or eastward flowing surface currents and sea ice. Compared to the western Siberian Arctic, dominated by the Barents Sea Ice Sheet, ice sheets of the eastern Siberian Arctic were small or stable with restricted fluctuations during the last glacial period (Knies et al., 2000, 2001; Svendsen et al., 2004). In particular the LGM appears to have been largely free of large ice sheets in Eastern Siberia (e.g. Polyak et al., 2000). Nonetheless, several increases of ice sheets extending to the shelves off eastern Severnaya Zemlya (Knies et al., 1999, 2000) and East Siberia (Müller, 1999) during MIS 6, 5d, 4 and to a lesser extent MIS 5b and 3 (Fig. 2h) may have additionally contributed to OC_{terr} input at site PC1 due to their relative proximity to the Chukchi Borderland. Furthermore, because the continental coast was halfway closer to site PC1 during late MIS 6 and MIS 2 (Fig. 1), erosion from the more exposed Chukchi Shelf may also have provided an OC_{terr} source during these periods.

5.4 Anti-correlation of CaCO₃ and TOC and their possible relation to oceanic and atmospheric circulation

The good positive correlation between $CaCO_3$ and the coarse fraction (Fig. 2c, d) is suggestive for a common source. Because the carbonate-rich Canadian Arctic should be viewed as the primary source of detrital carbonate, while carbonate is rare or absent on the Siberian margins and in the eastern Arctic Ocean (Bischof et al., 1996), we suggest that our more carbonate-rich and coarser samples would have mostly derived from the Canadian margins. In contrast, samples with low coarse fraction and lower carbonate could be explained by advection of organic carbon from carbonate-poor areas such as the Siberian margins, consistent with the results of Yamamoto and Polyak (2009), and/or by weakening of carbonate transport to the Northwind Ridge.

With regard to surface ocean current dynamics, Phillips and Grantz (2001) suggested that the relatively high detrital carbonate observed today at the Northwind Ridge would have been transported from the carbonate-rich Canadian Arctic via the Beaufort Gyre. Spielhagen (1997, 2004) also observed increases in carbonate at the southeastern Lomonosov Ridge during MIS 7 and middle MIS 5, which may have been related to substantial sediment transport via an extended Beaufort Gyre during warm periods (Phillips and Grantz, 2001). Thus, increases in detrital $CaCO_3$ at site PC1 were probably associated with enhanced advection of carbonate-rich sediments via sediment-laden sea ice and/or icebergs from the Canadian Arctic in association with an extended Beaufort Gyre during warm periods (Phillips and Grantz, 2001). On the other hand, during cold periods, which are associated with lower $CaCO_3$ contents and increased TOC at site PC1, the Beaufort Gyre would have contracted and the Transpolar Drift shifted towards North America (Bischof and Darby, 1997) (Fig. 1). We thus suggest that TOC increases observed at site PC1 derived from the Siberian ice sheets due to glacial erosion, at times when sediment input from the Canadian Arctic decreased due to a weaker Beaufort Gyre. The anti-correlation of $CaCO_3$ and TOC at site PC1 may therefore be related to a glacial-interglacial change in major Arctic Ocean current systems (Phillips and Grantz, 2001). Variable IRD and coarse fraction input at site PC1 provides additional evidence to such inference (Fig. 2a, c): increased IRD and coarse fraction contents during MIS 5e, 5c, 5a and partly MIS 3 were probably related to sea ice and/or iceberg advection by the Beaufort Gyre. In contrast, rather low IRD and coarse fraction contents during periods of large Eurasian ice sheets (Fig. 2a, c, h) would have been related to a weaker Beaufort Gyre and calm conditions with sea ice coverage over most of the year. Because dilution of TOC by $CaCO_3$ may also explain part of the anti-correlation of the two variables, changes in detrital carbonate supply in response to a changing Beaufort Gyre may have caused the observed temporal variations without invoking changes

in TOC. However, as mentioned in chapter 5.3, increases in organic matter input may be well expected in the area during cold periods (Yamamoto and Polyak, 2009) and therefore probably contributed to TOC increases.

Today, changes in Beaufort Gyre strength are coupled to the Arctic Oscillation (AO) (Thompson and Wallace, 1998): a negative AO is associated with an extended Beaufort Gyre, while a positive AO is associated with a contracted Beaufort Gyre and an extended cyclonic circulation over the Arctic Basin (Mysak, 2001; Rigor et al., 2002) (Fig. 1), involving the possibility that the dominant AO mode may have responded to changes in climate (Darby and Bischof, 2004).

5.5 Millennial-scale TOC and CaCO₃ variability in response to DOC and Bering Strait throughflow

TOC and $CaCO_3$ accumulation at site PC1 did not only respond to slow orbital-scale changes in global ice volume, but also varied at millennial scales, which might be related to abrupt variations in northern hemispheric temperature recorded in the NGRIP ice core, as based on a tentative temporal correlation of almost all DOS events between ~120 and ~45 ka BP with increases in TOC and in many cases with decreases in $CaCO_3$. Because atmospheric circulation responds immediately to hemispheric temperature changes, we suggest that one possible explanation for these millennial-scale variations in TOC and $CaCO_3$ are changes in AO and consequent changes in the Beaufort Gyre strength. In analogy to orbital-scale variations in Beaufort Gyre strength, discussed in chapter 5.4, a negative AO during interstadials would have generally led to a Beaufort Gyre extension decreasing OC_{terr} advection from the Siberian shelves and increasing $CaCO_3$ from the Canadian Arctic, while a positive AO during stadials would have led to a Beaufort Gyre contraction associated with increased OC_{terr} and lower $CaCO_3$ (Fig. 1).

During MIS 4 and the earlier part of MIS 3 (~70 to ~45 ka BP) TOC seems to have responded in a particularly sensitive manner to DOC, as it shows considerable relative increases during periods that might correspond to DOS 19, H6, DOS 15/16, 14 and H5. We suggest that TOC events at site PC1 were amplified during those periods in response to millennial-scale shallowing or closures of the Bering Strait during cold stadials of MIS 4 and 3 (Hu et al., 2010), which led to increases in coastal erosion along the new continuous coast line and inhibited dilution of Arctic water masses by Pacific waters. Both processes could have led to relative increases in OC_{terr} supply to the Chukchi Borderland. Our results suggest that the far western Arctic and Chukchi Sea areas were climatically not stable during the last glacial period, but experienced significant and abrupt changes possibly in association with northern hemispheric climate change and Bering Strait dynamics.

6 Summary and conclusion

In the present study we discussed orbital- and millennial-scale variations in TOC and $CaCO_3$ in the Chukchi Borderland in association with glacial-interglacial changes in ice volume and northern hemispheric temperature. We suggested that orbital- and millennial-scale increases of TOC in PC1 were related to glacial erosion during cold episodes of the last two glacial-interglacial cycles, while periods of increased $CaCO_3$ were related to advection of carbonate-rich sediments from the Canadian Arctic during warm episodes. We propose that this pattern, also in view of a tentative correlation between TOC events and DOS, could be explained by changes in dominant atmospheric surface pressure patterns expressed in mode shifts of the AO. A dominantly positive AO during glacial and stadial periods would have promoted a contracted Beaufort Gyre and an extended cyclonic circulation in the Arctic Ocean facilitating advection of OC_{terr} by the eastward flowing Atlantic Layer and/or eastward flowing surface currents and sea ice to the Northwind Ridge. A prevailing negative AO during warm episodes, on the other hand, would have promoted an extended and strengthened Beaufort Gyre associated with enhanced advection of detrital $CaCO_3$ by sea ice and icebergs to the Northwind Ridge. Observed TOC and $CaCO_3$ fluctuations in this study suggest that the Arctic responded sensitively to climate changes of the last two glacial-interglacial cycles on both orbital and millennial time scales through changes in oceanic and atmospheric circulation patterns, which supports scenarios of an amplified Arctic environmental change in response to modern climate change.

Edited by: Ö. Gustafsson

References

Backman, J., Jakobsson, M., Løvlie, R., Polyak, L., and Febo, L. A.: Is the central Arctic Ocean a sediment starved basin?, Quaternary Sci. Rev., 23, 1435–1454, 2004.

Belicka, L. L. and Harvey, H. R.: The sequestration of terrestrial organic carbon in Arctic Ocean sediments: a comparison and methods and implications for regional carbon budgets, Geochim. Cosmochim. Ac., 73, 6231–6248, 2009.

Bischof, J. F. and Darby, D. A.: Mid to Late Pleistocene ice drift in the western Arctic Ocean: evidence for a different circulation in the past, Science, 277, 74–78, 1997.

Bischof, J. F., Clark, D. L., and Vincent, J. S.: Pleistocene paleoceanography of the central Arctic Ocean: the sources of ice rafted debris and the compressed sedimentary record, Paleoceanography, 11, 743–756, 1996.

Braun, H., Christl, M., Rahmstorf S., Ganopolski, A., Mangini, A., Kubatzki, C., Roth, K., and Kromer, B.: Solar forcing of abrupt glacial climate change in a coupled climate system model, Nature, 438, 208–211, 2005.

Darby, D. A. and Bischof, J. F.: A Holocene record of changing Arctic Ocean ice drift, analogous to the effects of the Arctic Oscillation, Paleoceanography, 19, PA1027, doi:10.1029/2003PA000961, 2004.

Darby, D. A., Bischof, J. F., and Jones, G. A.: Radiocarbon chronology of depositional regimes in the western Arctic Ocean, Deep-Sea Res. Pt. II, 44(8), 1745–1757, 1997.

Dowdeswell, J. A., Elverhøi, A., and Spielhagen, R.: Glaciomarine sedimentary processes and facies on the Polar North Atlantic margins, Quaternary Sci. Rev., 17, 243–272, 1998.

Dowdeswell, J. A., Ó Cofaigh, C., Taylor, J., Kenyon, N. H., Mienert, J., and Wilken, M.: On the architecture of high-latitude continental margins: The influence of ice-sheet and sea-ice processes in the Polar North Atlantic, in: Glacier influenced sedimentation on high-latitude continental margins, edited by: Dowdeswell, J. A. and Ó Cofaigh, C., Geological Society of London (Special Publication), 203, 33–54, 2002.

Elverhøi, A., Dowdeswell, J. A., Funder, S., Mangerud, J., and Stein, R.: Glacial and oceanic history of the Polar North Atlantic margins, Quaternary Sci. Rev., 17, 1–10, 1998.

Hemming, S. R.: Heinrich events: Massive late Pleistocene detritus layers of the North Atlantic and their global climate imprint, Rev. Geophys., 42, RG1005, doi:10.1029/2003RG000128, 2004.

Hu, A., Meehl, G. A., Otto-Bliesner, B. L., Waelbroeck, C., Han, W., Loutre, M.-F., Lambeck, K., Mitrovica, J. X., and Rosenbloom, N.: Influence of Bering Strait flow and North Atlantic circulation on glacial sea-level changes, Nat. Geosci., 729(3), 118–121, 2010.

Johannessen, O. M., Bengtsson, L., Miles, M. W., Kuymina, S. I., Semenov, V. A., Alekseev, G. V., Nagurnyi, A. P., Yakharov, V. F., Bobylev, L. P., Petterson, L. H., Hasselmann, K., and Cattle, H. P.: Arctic climate change, observed and modelled temperature and sea-ice variability, Tellus, 56A(4), 328–341, 2004.

Josenhans, H. W., Zevenhuizen, J., and Klassen, R. A.: The Quaternary geology of the Labrador Shelf, Can. J. Earth Sci., 23, 1190–1213, 1986.

Knies, J., Vogt, C., and Stein, R.: Late quaternary growth and decay of the Svalbard-Barents-Sea ice sheet and paleoceanographic evolution in the adjacent Arctic Ocean, Geo-Mar. Lett., 18, 195–202, 1999.

Knies, J., Müller, C., Nowaczyk, N., Vogt, C., and Stein, R.: A multiproxy approach to reconstruct the environmental changes along the Eurasian continental margin over the last 150000 years, Mar. Geol., 163, 317–344, 2000.

Knies, J., Kleiber, H. P., Matthiessen, J., Müller, C., and Nowaczyk, N.: Marine ice-rafted debris records constrain maximum extent of Saalian and Weichselian ice-sheets along the northern Eurasian margin, Global Planet. Change, 31, 45–64, 2001.

Lisiecki, L. E. and Raymo, M. E.: A Pliocene-Pleistocene stack of 57 globally distributed benthic δ18O records, Paleoceanography, 20, PA1003, doi:10.1029/2004PA001071, 2005.

Macdonald, R. W., Solomon, S. M., Cranston, R. E., Welch, H. E., Yunker, M. B., and Gobeil, C.: A sediment and organic carbon budget for the Canadian Beaufort Shelf, Mar. Geol., 144, 255–273, 1998.

Macdonald, R. W., Harner, T., Fyfe, J., Loeng, H., and Weingartner, T.: AMAP Assessment 2002: The influence of global change on contaminant pathways to, within, and from the Arctic, Arctic Monitoring and Assessment Programme (AMAP), Scientific Report, Oslo, 65 pp., 2003.

McCorkle, D. C., Bruce, H., Corlis, S., and Farnham, C. A.: Vertical distributions and stable isotopic compositions of live (stained) benthic foraminifera from the North Carolina and California continental margins, Deep-Sea Res. Pt. I, 44, 983–1024, 1997.

Müller, C.: Rekonstruktion der Paläo-Umweltbedingungen am Laptev-See-Kontinentalrand während der beiden letzten Glazial-/Interglazial-Zyklen anhand sedimentologischer und mineralogischer Untersuchungen, Report on Polar Research, 328, 146 pp., 1999.

Mysak, L. A.: Patterns of Arctic circulation, Science, 293, 1269–1270, 2001.

Naidu, A. S., Cooper, L. W., Grebmeier, J. M., Whitledge, T. E., and Hameedi, M. J.: The continental margin of the North Bering-Chukchi Sea: Distribution, sources, fluxes, and burial rates of organic carbon, in: The organic carbon cycle in the Arctic Ocean, edited by: Stein, R. and Macdonald, R. W., Heidelberg, Springer-Verlag, 193–203, 2004.

NGRIP members: High-resolution record of Northern Hemisphere climate extending into the last interglacial period, Nature, 431, 147–151, 2004.

Phillips, R. L. and Grantz, A.: Quaternary history of sea ice and paleoclimate in the Amerasia Basin, Arctic Ocean, as recorded in the cyclical strata or Northwind Ridge, Geol. Soc. Am. Bull., 109, 1101–1115, 1997.

Phillips, R. L. and Grantz, A.: Regional variations in provenance and abundance of ice-rafted clasts in Arctic Ocean sediments: Implications for the configuration of Late Quaternary oceanic and atmospheric circulation in the Arctic, Mar. Geol., 172, 91–115, 2001.

Polyak, L. V., Gataullin, V., Epshtein, O., Okuneva, O., and Stelle, V.: New constraints on the limits of the Barents-Kara ice sheet during the Last Glacial Maximum based on borehole stratigraphy from the Pechora Sea, Geology, 28, 611–614, 2000.

Polyak, L. V., Curry, W. B., Darby, D. A., Bischof, J., and Cronin, T. M.: Contrasting glacial/interglacial regimes in the Western Arctic Ocean as exemplified by a sedimentary record from the Mendeleev Ridge, Palaeogeogr. Palaeoclim. Palaeoecol., 203, 73–79, 2004.

Rachold, V., Grigoriev, M. N., Are, F. E., Solomon, S., Reimnitz, E., Kassens, H., and Antonow, M.: Coastal erosion vs riverine sediment discharge in the Arctic shelf seas, Int. J. Earth Sci., 89, 450–460, 2000.

Reimer, P. J., Baillie, M. G. L., Bard, E., Bayliss, A., Beck, J. W., Blackwell, P. G., Bronk Ramsey, C., Buck, C. E., Burr, G. S., Edwards, R. L., Friedrich, M., Grootes, P. M., Guilderson, T. P., Hajdas, I., Heaton, T. J., Hogg, A. G., Hughen, K. A., Kaiser, K. F., Kromer, B., McCormac, F. G., Manning, S. W., Reimer,

R. W., Richards, D. A., Southon, J. R., Talamo, S., Turney, C. S. M., van der Plicht, J., and Weyhenmeyer, C. E.: IntCal09 and Marine09 radiocarbon age calibration curves, 0-50000 years cal BP, Radiocarbon, 51, 1111–1150, 2009.

Reimnitz, E., Graves, S. M., and Barnes, P. W.: Beaufort Sea coastal erosion, sediment flux, shoreline evolution and the erosional shelf profile, U.S. Geological Survey, Map I-1182-G, 22 pp., 1988.

Rigor, I. G., Wallace, J. M., and Colony, R. L.: On the response of sea ice to the Arctic Oscillation, J. Climate, 15, 2648–2668, 2002.

Shipp, S. S., Wellner, J. S., and Anderson, J. B.: Retreat signature of a polar ice stream: Sub-glacial geomorphic features and sediments from the Ross Sea, Antarctica, in: Glacier influenced sedimentation on high-latitude continental margins, edited by: Dowdeswell, J. A. and Ó. Cofaigh, C., Geological Society of London (Special Publication 203), 277–304, 2002.

Spielhagen, R. F., Bonani, G., Eisenhauer, A., Frank, M., Frederichs, T., Kassens, H., Kubik, P. W., Mangini, A., Nörgaard-Pedersen, N., Nowaczyk, N. R., Schäper, S., Stein, R., Thiede, J., Tiedemann, R., and Wahsner, M.: Arctic Ocean evidence for Late Quaternary initiation of northern Eurasian ice sheets, Geology, 25, 783–786, 1997.

Spielhagen, R. F., Baumann, K.-H., Erlenkeuser, H., Nowaczyk, N. R., Nørgaard-Pedersen, N., Vogt, C., and Weiel, D.: Arctic Ocean deep-sea record of Northern Eurasian ice sheet history, Quaternary Sci. Rev., 23(11–13), 1455–1483, 2004.

Stein, R.: Arctic Ocean Sediments: Processes, Proxies, and Paleoenvironment, Developments in Marine Geology, Elsevier, Amsterdam, 2, 592 pp., 2008.

Stein, R. and Korolev, S.: Shelf-to-basin sediment transport in the eastern Arctic Ocean, Report on Polar Research, 144, 87–100, 1994.

Stuiver, M. and Reimer, J.: Extended 14C data base and revised CALIB 3.0 14C age calibration program, Radiocarbon, 35, 215–230, 1993.

Svendsen, J. I., Alexanderson, H., Astakhov, V. I., Demidov, I., Dowdeswell, J. A., Funder, S., Gataullin, V., Henriksen, M., Hjort, C., Houmark-Nielsen, M., Hubberten, H. W., Ingolfsson, O., Jakobsson, M., Kjaer, K. H., Larsen, E., Lokrantz, H., Lunkka, J. P., Lysa, A., Mangerud, J., Matiouchkov, A., Murray, A., Moller, P., Niessen, F., Nikolskaya, O., Polyak, L., Saarnisto, M., Siegert, C., Siegert, M. J., Spielhagen, R. F. and Stein, R.: Late quaternary ice sheet history of northern Eurasia, Quaternary Sci. Rev., 23, 1229–1272, 2004.

Thompson, D. W. J. and Wallace, J. M.: The Arctic Oscillation signature in the wintertime geopotential height and temperature fields, Geophys. Res. Lett., 29(9), 1297–1300, 1998.

Uchida, M., Shibata, Y., Yoneda, M., and Morita, M.: Technical progress in AMS microscale radiocarbon analysis for molecular-level biogeochemical studies, Nucl. Instr. and Meth. in Phys. Res. B, 223/224, 313–317, 2004.

Uchida, M., Shibata, Y., Ohkushi, K., Yoneda, M., Kawamura, K., and Morita, M.: Age discrepancy between molecular biomarkers and calcareous foraminifera isolated from the same horizons of Northwest Pacific sediments, Chem. Geol., 218, 73–89, doi:10.1016/j.chemgeo.2005.01.026, 2005.

Uchida, M., Ohkushi, K., Kimoto, K., Inagaki, F., Ishimura, T., Tsunogai, U., TuZino, T., and Shibata, Y.: Radiocarbon-based

carbon source quantification of anomalous isotopic foraminifera in last glacial sediments in the western North Pacific, Geochem. Geophys. Geosys., 9, Q04N14, doi:10.1029/2006gc001558, 2008.

Winkelmann, D.: Sediment dynamics of megaslides along the Svalbard continental margin and the relation to paleoenvironmental changes and climate history, unpublished Ph.D. thesis, Bremen University, 180 pp., 2007.

Winkelmann, D., Schäfer, C., Stein, R., and Mackensen, A.: Terrigenous events and climate history within the Sophia Basin, Arctic Ocean, Geochem. Geophy. Geosy., 9, Q07023, doi:10.1029/2008GC002038, 2008.

Wollenburg, J. E. and Mackensen, A.: Living benthic foraminifers from the central Arctic Ocean: Faunal composition, standing stock and diversity, Mar. Micropaleontol., 34, 153–185, 1998.

Yamamoto, M. and Polyak, L.: Changes in terrestrial organic matter input to the Mendeleev Ridge, western Arctic Ocean, during the Late Quaternary, Global Planet. Change, 68, 30-37, 2009.